

# Glass-ceramic for low temperature co-fired dielectric ceramic materials based on $\text{La}_2\text{O}_3\text{--B}_2\text{O}_3\text{--TiO}_2$ glass with BNT ceramics

Byung-Hae Jung, Seong-Jin Hwang, Hyung-Sun Kim\*

Department of Materials Science and Metallurgical Engineering, Sunchon National University, 315 Maegok-dong, Sunchon 540-742, South Korea

Received 7 March 2004; received in revised form 5 July 2004; accepted 10 July 2004

Available online 11 September 2004

## Abstract

Low-temperature co-fired ceramic (LTCC) materials with a sintering temperature of  $<900^\circ\text{C}$  were developed using rare earth derived borate glass ( $\text{La}_2\text{O}_3\text{--B}_2\text{O}_3\text{--TiO}_2$ ) and a conventional BNT ( $\text{BaO--Nd}_2\text{O}_3\text{--TiO}_2$ ) ceramic. The sintering behavior, phase evaluation, sintered morphology, and microwave dielectric properties were investigated. It was found that increasing the sintering temperature from  $750$  to  $850^\circ\text{C}$  led to increases in shrinkage and microwave dielectric properties ( $\approx 20$  for  $\epsilon_r$  and  $>8000$  GHz for  $Q^*f_0$ ) but a decrease in porosity. The final crystal phases of the sintered samples were identified as HT- $\text{LaBO}_3$  and  $\text{TiO}_2$ .

© 2004 Elsevier Ltd. All rights reserved.

**Keywords:** Sintering; Glass-ceramic; Dielectric properties; LTCC; Borate glass;  $\text{BaNd}_2\text{Ti}_5\text{O}_{14}$

## 1. Introduction

Due to the limited sintering temperature capability of metal electrodes such as Ag or Cu, low temperature co-fired ceramics (LTCCs) with sintering temperature below  $900^\circ\text{C}$  have been in great demand. LTCCs are also of great importance to the electronic industry for building smaller RF modules, and fulfilling the necessity for miniaturization of devices in the wireless communication industry.<sup>1–6,12–14</sup> However, most of the known commercial ceramic materials possessing a high quality factor and large dielectric constant usually need high sintering temperatures.<sup>16–18</sup> To solve this problem, oxide type powders such as  $\text{B}_2\text{O}_3$ ,  $\text{SiO}_2$  and  $\text{Li}_2\text{O}$  and low-melting glass frits are generally mixed with ceramic materials to reduce the sintering temperature to below  $900^\circ\text{C}$  as is required.<sup>5,7,8</sup> Typical glass systems for low-melting are borosilicate and lead borosilicate glasses. However, if the amount of frit is large the network formers contained in the remaining glass materials such as  $\text{B}_2\text{O}_3$  and  $\text{SiO}_2$  can profoundly absorb the microwave power at high frequen-

cies, causing degradation of the quality factor of the final materials.<sup>1,7</sup>

Compared with liquid phase sintering and low-melting glass frits in which the glass phase remains, another approach using a ‘glass-ceramic’ produces different results since glass frits crystallize during the sintering stage. The advantages offered by this glass-ceramic approach include shape stability after sintering, improved dielectric properties, mechanical strength and controlled thermal expansivity.<sup>2,3,10</sup> Although there are some previous studies related to the use of glass-ceramic for LTCC materials, these studies are mostly focused on the substrate materials which possess a low dielectric constant ( $<10$ ).<sup>4,9</sup> There are few studies concerning the use of glass-ceramic materials with a mid-range dielectric constant ( $>15$ ).<sup>7,10,11</sup>

Given this background with glass-ceramics, in this study the glass composition  $\text{La}_2\text{O}_3\text{--B}_2\text{O}_3\text{--TiO}_2$ , as an alternative glass composition, and commercial  $\text{BaNd}_2\text{Ti}_5\text{O}_{14}$  as a ceramic material were used. The sintering characteristic of this composite, the mechanism of how the glass and ceramic materials interact with each other under different sintering conditions and finally how the microstructure of the sintered composites affects the dielectric properties are discussed in detail.

\* Corresponding author. Tel.: +82 61 750 3555; fax: +82 61 750 3550.  
E-mail address: [hskim@sunchon.ac.kr](mailto:hskim@sunchon.ac.kr) (H.-S. Kim).

## 2. Experimental procedure

The starting ceramic material used was a commercial BNT ( $\text{BaO-Nd}_2\text{O}_3\text{-TiO}_2$ ) ceramic powder (MBRT90, Fuji Titanium Ind. Japan,  $d_{50}$ : 2.9  $\mu\text{m}$ ), which was found to be thermally stable in the single  $\text{BaNd}_2\text{Ti}_5\text{O}_{14}$  phase using XRD (X-Ray Diffractometer, Philips, X'PERT).<sup>15</sup> The raw materials for the glass frit were  $\text{La}_2\text{O}_3$ ,  $\text{H}_3\text{BO}_3$  and  $\text{TiO}_2$  which all have high purity (Aldrich, USA). The batches were melted in a platinum crucible at 1300 °C for 1 h. The glass melt was quickly poured and quenched on a copper plate and pulverized in a vibration mill for 4 h (mean diameter: 6–8  $\mu\text{m}$ ). For the preparation of bulk specimens, the melts from the furnace were poured into a graphite mould and heated to the temperature of 10 °C above the glass transition temperature ( $T_g$ ) of each glass. The mould was then moved back into the furnace to anneal the glass for 1 h and then cooled very slowly in the furnace. The glass powder (60 wt.%) and ceramic materials (40 wt.%) were mixed by a ball mill for 48 h and then dried for making pellets (1.5 cm in diameter and 8 cm in height) by cold isostatic pressing (under 200 MPa). The pellets were sintered in the temperature range of 750–900 °C for 10–120 min at a heating rate of 10 °C/min.

The bulk density of the sintered samples was determined by the Archimedes method. The glass transition temperature ( $T_g$ ) and crystallization peak ( $T_p$ ) were determined with a differential thermal analyzer (DTA-TA 1600, TA Instruments, USA) under 10 °C/min heating rate. From the glass, Glass fibers of 0.5–0.75 cm in diameter and 23.5 cm in length were made for the test of  $T_s$  (Littleton softening point); the point at which the fiber elongates under its own weight at a rate of 1 mm/min. The thermal expansion coefficient was examined by TMA (TA Instruments). The shrinkage rate of the samples was determined by samples diameter before and after sintering. The porosity was measured by automated mercury porosimeter (AutoPore IV 9510, Micromeritics, USA). The microstructure of the thermally etched samples was examined using a scanning electron microscope (SEM, HITACHI, Japan) and Energy Dispersive X-Ray Microanalysis System (EDAX, Phoenix60). The microwave dielectric properties of glass was measured by impedance analyzer (4194Es, Agilent, USA) at 1 MHz and network analyzer (8720Es, Agilent, USA) at 4.7 GHz. The microwave dielectric properties of glass/ceramic was measured by network analyzer (8720Es, Agilent, USA) at 7–8 GHz.

## 3. Results and discussion

### 3.1. Characteristics of glass ( $\text{La}_2\text{O}_3\text{-B}_2\text{O}_3\text{-TiO}_2$ )

The formation of all glasses studied, based on  $\text{La}_2\text{O}_3\text{-B}_2\text{O}_3\text{-TiO}_2$  ternary system is given in Table 1. For glass forming, glasses with smaller amounts of the glass former  $\text{B}_2\text{O}_3$  (below 55 mol%) could not be made because of fast devitrification during quenching. Also the amount of

Table 1

Compositions of melts  $\text{La}_2\text{O}_3\text{-B}_2\text{O}_3\text{-TiO}_2$  glass system (in mol%) melting at 1300 °C for 1 h and the results of glass state after quenching at room temperature

Glass no.	$\text{La}_2\text{O}_3$	$\text{B}_2\text{O}_3$	$\text{TiO}_2$	Notes
L1	20	40	40	Crystallized
L2 <sup>a</sup>	20	60	20	Glassy
L3	20	55	25	Glassy
L4	20	50	30	Glassy
L5	25	60	15	Glassy
L6	25	55	20	Glassy
L7	30	40	30	Crystallized
L8	20	35	45	Crystallized
L9	25	35	40	Crystallized
L10	25	30	45	Crystallized
L11	10	50	40	No melting
L12	15	50	35	Partially crystallized

<sup>a</sup> Glass composition which was used in this study.

$\text{TiO}_2$  had to be limited to below 30 mol% for glass formation. Among these glasses,  $20\text{La}_2\text{O}_3\cdot 60\text{B}_2\text{O}_3\cdot 20\text{TiO}_2$  (in mol%) was chosen for the present experiment, which was then mixed with BNT ceramic powder.

To confirm whether the glass frits could properly fuse with the ceramic materials while keeping the temperature below 900 °C (as required) needed several additional thermal results of the glass to be considered. The DTA result of L2 ( $20\text{La}_2\text{O}_3\cdot 60\text{B}_2\text{O}_3\cdot 20\text{TiO}_2$  (in mol%)) glass in Fig. 1 shows that an exothermal peak indicating crystallization occurred at a higher temperature with increasing frit size. The crystallization of the glass resulted from surface crystallization rather than bulk crystallization in the glass system, which can be seen in Fig. 2. The crystal growth rate dramatically increased as the temperature increased (Fig. 2). The glass transition temperature ( $T_g = 657$  °C) of L2 glass was found at the same temperature for all frit sizes. The glass also showed the Littleton softening point ( $T_s, \eta = 10^{7.6}$  dPa) at 722 °C and the melting point at 1043 °C. The thermal expansion coefficient was  $7.6 \times 10^{-7} \text{ K}^{-1}$  and dielectric constant was 12–13 (Table 2).

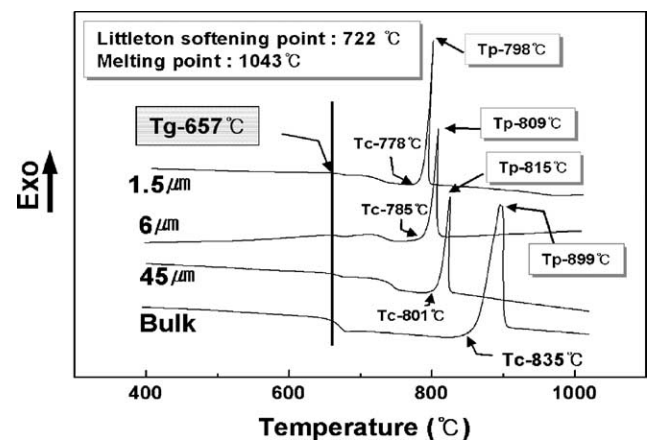


Fig. 1. DTA curves for different frit sizes heated at 10 °C/min heating rate. ( $T_g$ , glass transition temperature;  $T_c$ , onset point of crystallization;  $T_p$ , peak crystallization temperature.)

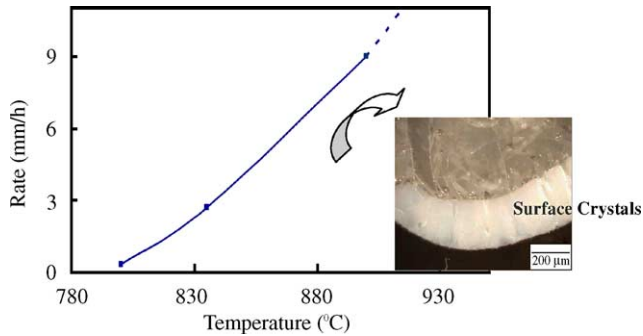


Fig. 2. Surface crystal growth rate at different heating temperatures and the image of surface crystal appearing in a bulk glass.

Table 2  
Dielectric and thermal characteristics of L2 glass

Characteristic	Dielectric constants		CTE ( $\times 10^{-6} \text{ K}^{-1}$ )	$T_s$ ( $^{\circ}\text{C}$ )	$T_m$ ( $^{\circ}\text{C}$ )
	At 1 MHz	At 4.7 GHz			
L2	12.6	11.5	7.4	722	1043

The overall conclusion regarding this LBT glass composition is that the glass showed a low viscosity characteristic, as shown by low  $T_g$  and  $T_s$  points, and suitable crystallization for LTCC application as crystallized glass. Particularly regarding the lower  $T_s$  point of the glass than the required sintering temperature for LTCCs ( $\sim 900^{\circ}\text{C}$ ), this glass can critically aid the sinterability of the composites. Compared to silicate and borosilicate glasses, the relatively higher dielectric constant of bulk glass ( $\epsilon_r > 10$ ) could be beneficial for dielectric properties, notwithstanding the possibility for crystallization of the glass.

### 3.2. Properties of co-fired glass/ceramics

As shown in Fig. 3, the shrinkage of the L2 glass/ceramic (BNT) rapidly increased until the temperature reached

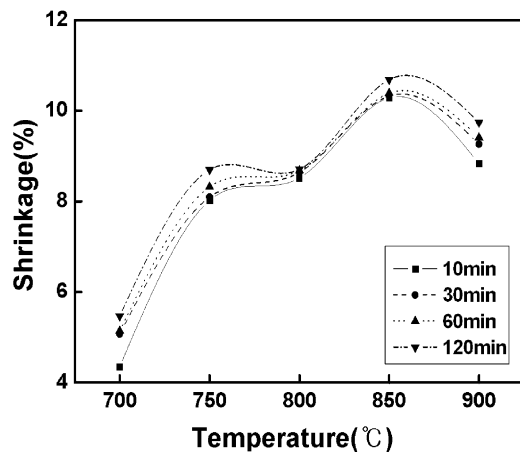


Fig. 3. Shrinkage of glass-ceramic composites as a function of sintering temperature and under different sintering times.

$850^{\circ}\text{C}$ , thereafter it slightly decreased. There was no significant difference in the shrinkage with different sintering times. This suggests that the reactions such as a rearrangement, crystallization and diffusion between glass frit and the ceramic material were dependent on the significant temperature ( $T_g$ ,  $T_s$  and  $T_p$ ). The significant increase of shrinkage can be explained together with the change of microstructure and decrease in porosity as the temperature increased. In Table 4, the porosity at  $750$  and  $800^{\circ}\text{C}$  was about 15% but it became noticeably smaller (5%) at up to  $850^{\circ}\text{C}$  because the low glass viscosity would be the effect.

According to the DTA result in Fig. 4, a different profile of the mixture of glass and ceramic was obtained compared to the previous, glass only, thermal analysis (Fig. 1). There are three recognizable exothermic peaks at  $767$ ,  $803$  and  $850^{\circ}\text{C}$ , respectively, unlike the one exothermic peak for glass. These three peaks are related to the occurrence of three crystal phases. The XRD analysis data showed that the first peak occurred at the formation of the low temperature forming LT-LaBO<sub>3</sub> phase (JCPDS no. 72-0074), the second was for the high temperature forming HT-LaBO<sub>3</sub> phase (JCPDS no. 12-0762) and the third was for the TiO<sub>2</sub> phase (JCPDS no. 76-0649).

To study the interaction between LBT glass materials and BNT ceramics (60:40 wt.%), the mixture was well mixed and then sintered at  $750$ – $900^{\circ}\text{C}$  for 1 h. There had to be two initial phases such as glass and ceramic phases at room temperature but as the samples underwent sintering, different phases were formed. At lower temperatures ( $<750^{\circ}\text{C}$ ), the glass started to fuse causing slight shrinkage and then, until the temperature reached the starting point of crystallization ( $T_c = 750^{\circ}\text{C}$ ), the fused glass worked as a typical liquid-phase sintering aid, coating the ceramic materials.

As shown in the thermally etched microstructure images (Fig. 5), it seems that a small reaction had already started at  $750^{\circ}\text{C}$  and occurred more rigorously after  $850^{\circ}\text{C}$ . At temperatures of  $750$ – $800^{\circ}\text{C}$ , grain sizes were relatively small compared with the specimens sintered at higher temperatures ( $850$ – $900^{\circ}\text{C}$ ) because of the relatively poor reaction between glass and ceramic. However, grains became larger as the temperature increased.

In the magnified backscattered images (Fig. 6) and EDX analysis (Table 3), the black area labeled A indicates a TiO<sub>2</sub>-rich ceramic while the white area labeled B represents complicated phases which were composed of glass and dissolved ceramic. In the case of the black area (A), La, B and Ti ions were dominant and Bi, Ba and Nd remained as minor components. The byproduct of the reaction between glass and ceramic materials should be the phase labeled B (white area).

Table 3  
The EDX analyses for regions A and B in Fig. 6

Elements	O	Ti	Nd	Bi	Ba	B	La	Total
A (black area)	69.57 <sup>a</sup>	27.18	2.68	0.57	–	–	–	
B (white area)	25.31	6.32	1.69	0.12	0.83	65.08	2.65	

<sup>a</sup> Values are in at.%.

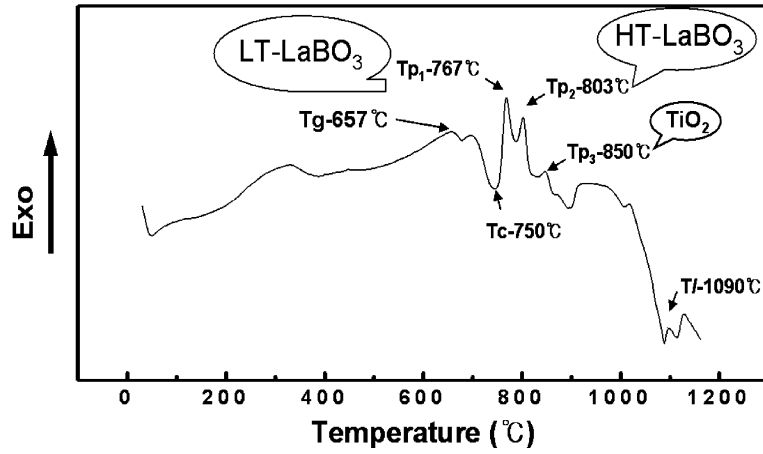


Fig. 4. DTA result of glass-ceramic composite heated at 10 °C/min heating rate.

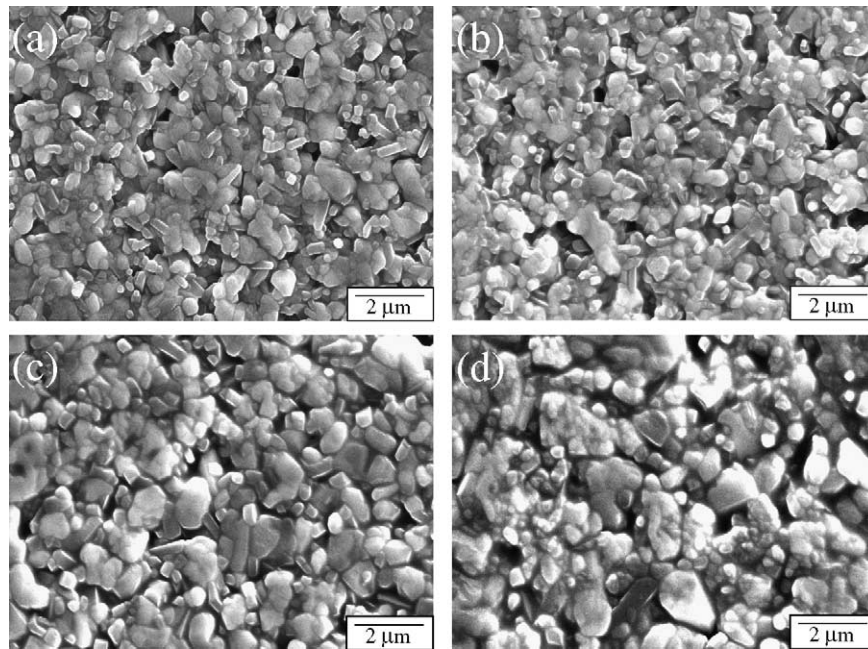


Fig. 5. SEM images of glass-ceramic composites after sintering at different temperature: (a) 750 °C, (b) 800 °C, (c) 850 °C and (d) 900 °C.

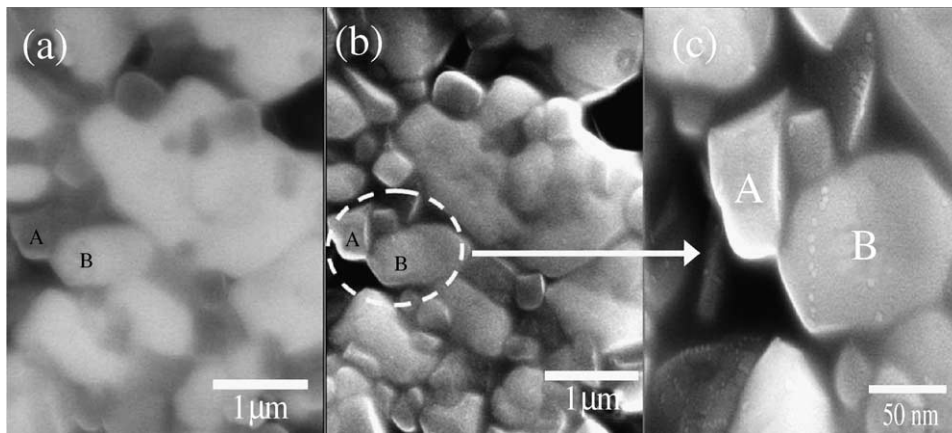


Fig. 6. Back scattered (a), normal secondary electron (b) and magnified image (c) of a glass-ceramic composite after 850 °C firing.

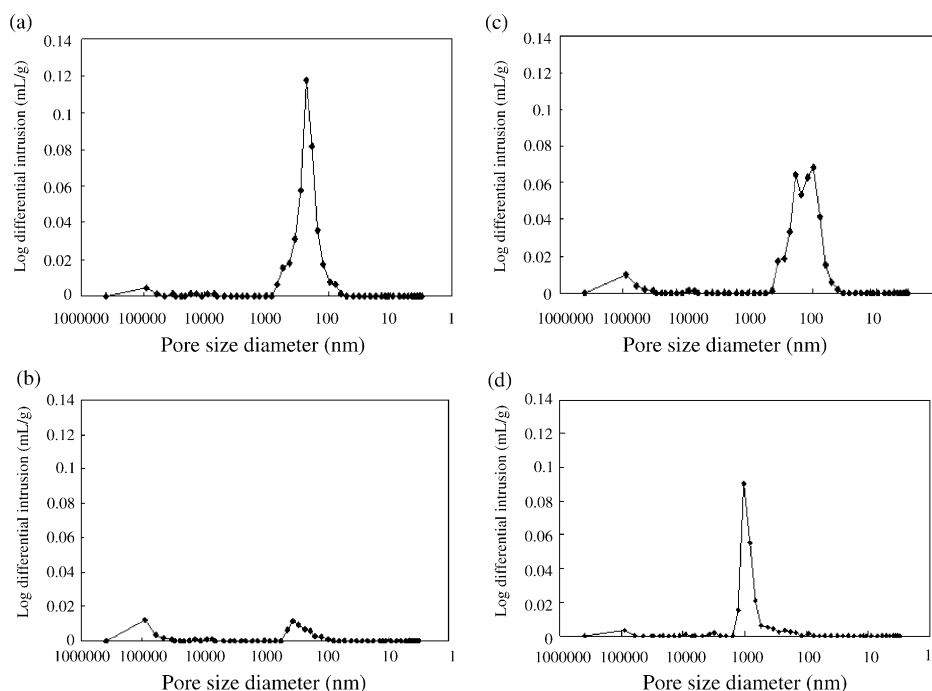


Fig. 7. Pore size distribution of sintered glass-ceramic composites: (a) 750 °C, (b) 800 °C, (c) 850 °C and (d) 900 °C.

It seems that Ba and Nd from the ceramic components (Ba, Nd, Ti, and O) migrate to the glass matrix and play as key elements to form a new phase.

Regarding porosity and pore size distribution, as the sintering temperature increased the intrusion of Hg gradually decreased, which meant the rapid reduction of porosity in the sintered samples (Fig. 7). However, interestingly, large pores over 100  $\mu\text{m}$  appeared at 800 and 850 °C as shown in Fig. 7b and c. The formation of larger pores at high temperature resulted from vigorous crystallization of glass frits at high temperature.

The density of the composites (sintered samples) ranged from 4.0 to 4.2  $\text{g}/\text{cm}^3$  (Table 4), which was a comparatively low value compared to the density of the pure ceramic material (5.6  $\text{g}/\text{cm}^3$ ). The slight decrease in density as the sintering temperature increased (Table 4) can be explained by the formation of phases with lower density (Table 5). Assuming that the microstructure of the sintered samples at 850 °C is composed of 50% of HT  $\text{LaBO}_3$ , 50% of  $\text{TiO}_2$  and 5% of porosity and at 750 °C, 40% of LT- $\text{LaBO}_3$ , 40% of ceramic ( $\text{BaNd}_2\text{Ti}_5\text{O}_{14}$ ) and 20% of glass with 5% of porosity based on results of the density and porosity, theoretically the predicted densities based on Table 5 give 4.3 and 4.0  $\text{g}/\text{cm}^3$  for 750 and 850 °C, respectively, as the experimental appar-

ent densities revealed lower values 4.266 and 4.059  $\text{g}/\text{cm}^3$  in Table 4.

The XRD results, in Fig. 8, made it clear that the crystal from glass only ( $\text{LaB}_3\text{O}_6$ ) was completely different from crystals from glass/ceramic composites ( $\text{LaBO}_3$ ). As far as glass/ceramic composites are concerned, at 750 °C various phases existed including ceramic phase, low temperature forming LT- $\text{LaBO}_3$  and amorphous (glassy) phase which was not yet crystallized. As the temperature increased to 800 °C, LT- $\text{LaBO}_3$  completely changed to high temperature forming HT- $\text{LaBO}_3$  and a different type of ceramic phase was formed. Finally, at 850–900 °C, HT- $\text{LaBO}_3$  emerged as the main phase and a small amount of  $\text{TiO}_2$  phase was detected.

Table 6 shows the dielectric properties of the composites; the dielectric constant ranged from approximately 18–20 with no significant change was shown with an increasing sintering temperature. However, quality factor and temperature coefficient (TCF) both gradually increased with the increasing temperature. The sudden decrease in the quality factor at 900 °C can be ascribed to the extreme grain growth and increase of porosity at this temperature (Figs. 5 and 7).

Table 4  
Properties of sintered glass-ceramic composites

Sintered samples	Apparent density ( $\text{g}/\text{cm}^3$ )	Porosity (%)
At 750 °C	4.266	15.1
At 800 °C	4.065	15.6
At 850 °C	4.059	5.1
At 900 °C	4.001	8.9

Table 5  
Comparison of density of crystal phases

Phases	JCPDS no.	Density ( $\text{g}/\text{cm}^3$ )
LT- $\text{LaBO}_3$	72-0074	5.107
HT- $\text{LaBO}_3$	12-0736	5.304
$\text{Nd}_4\text{TiO}_{24}$	33-0943	5.171
$\text{TiO}_2$ (rutile)	76-0649	4.251
$\text{LaB}_3\text{O}_6$	72-2095	4.189
Ceramic ( $\text{BaNd}_2\text{Ti}_5\text{O}_{14}$ )	33-0166	5.643
Pure glass		4.058

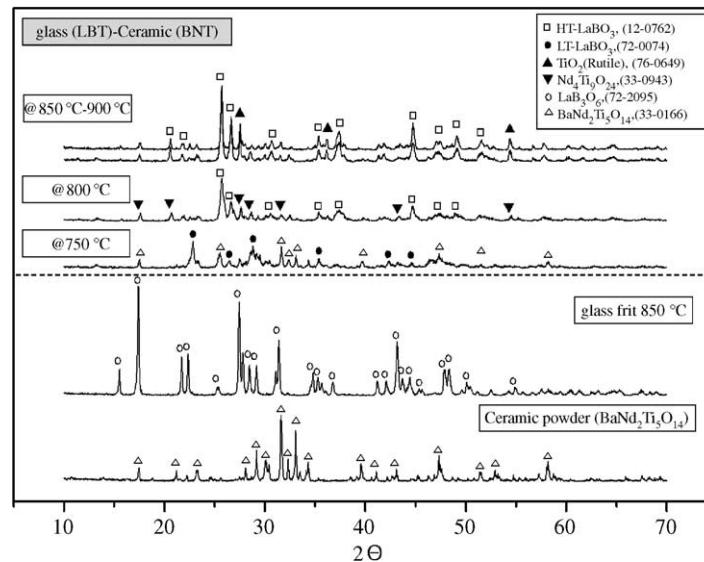


Fig. 8. X-ray diffraction patterns showing different phases according to the material and sintering temperature.

The change of dielectric constant is attributed to the crystal phases occurrence particularly the HT-LaBO<sub>3</sub> phase. Unlike the dielectric constant, it is well known that the quality factor (reciprocal of dielectric loss) is primarily a response to the network structure of the remnant glass phase<sup>4</sup> and mostly affected by porosity, because the pores in the microstructure increase dielectric loss. At 750 °C, the quality factor was lower than for the others because the remaining amorphous phase affected the quality factor. At the higher firing temperature a higher quality factor was obtained since the increase in firing temperature removed the remaining amorphous phase, resulting in more reaction between the glass and ceramic materials and the formation of a second phase (LaBO<sub>3</sub> and TiO<sub>2</sub> phases). As shown in Table 6, the highest quality factor was obtained at 850 °C because of the highest shrinkage (Fig. 3) and the lowest porosity (Table 3). Thus 850 °C could be described as the optimized sintering temperature.

This study is a preliminary investigation of the LBT glass and BNT ceramic composite material and will be continued

by bringing in different ceramic materials, in order to achieve more applicable microwave dielectric properties.

#### 4. Conclusion

The glass-ceramic based on La<sub>2</sub>O<sub>3</sub>–B<sub>2</sub>O<sub>3</sub>–TiO<sub>2</sub> (LBT) glass composition was used as an alternative LTCC material after mixing with commercial BaO–Nd<sub>2</sub>O<sub>3</sub>–TiO<sub>2</sub> (BNT) based ceramic material. Through the sintering process, one of the most significant sintering behaviors was the formation of HT-LaBO<sub>3</sub> and TiO<sub>2</sub> as final phases reacted between the BNT ceramic and LBT glass. The products played positively to improve the microwave dielectric properties of BNT ceramic. As a result, the sintering temperature of the commercial BNT ceramic could be reduced to 850 °C with the composite and the microwave dielectric properties were 20 for  $\epsilon_r$ , 8000 for  $Q^*f_0$  (GHz) and 76.8 for TCF at 6–7 GHz. The results suggested the composite could be an optimal LTCC dielectric material.

Table 6

Microwave dielectric properties of sintered pure ceramic and glass/ceramic composites and phases at different temperature

Samples	Microwave dielectric properties		
	$\epsilon_r$	$Q^*f_0$ (GHz)	$\tau_{cf}$
Pure ceramic <sup>a</sup> (BaNd <sub>2</sub> Ti <sub>5</sub> O <sub>14</sub> )	90	6100	3.62
G/C			
750 °C <sup>b</sup> (BaNd <sub>2</sub> Ti <sub>5</sub> O <sub>14</sub> , LT-LaBO <sub>3</sub> , glass) <sup>c</sup>	18.4	2023	11.06
800 °C (Nd <sub>4</sub> TiO <sub>24</sub> , HT-LaBO <sub>3</sub> )	18.1	5542	42.7
850 °C (TiO <sub>2</sub> , HT-LaBO <sub>3</sub> )	19.9	8218	76.8
900 °C (TiO <sub>2</sub> , HT-LaBO <sub>3</sub> )	19.6	6160	85.9

<sup>a</sup> Sintered at 1300 °C for 2 h.

<sup>b</sup> Sintering temperature.

<sup>c</sup> Existing phases.

#### Acknowledgements

This work was supported by grant no. R01-2002-000-00260-02003 from the Basic Research Program of the Korea Science Engineering Foundation.

#### References

- Cheng, C. C., Hsieh, T. E. and Lin, I. N., The effect of composition on Ba–Nd–Sm–Ti–O microwave dielectric materials for LTCC application. *J. Eur. Ceram. Soc.*, 2003, **23**, 119–123.
- Jantunen, H., Rautioaho, R., Uusimäki, A. and Leppavuori, S., Compositions MgTiO<sub>3</sub>–CaTiO<sub>3</sub> ceramic with two borosilicate glasses

- for LTCC technology. *J. Eur. Ceram. Soc.*, 2000, **20**, 2331–2336.
3. Chen, C. S., Chou, C. C., Chen, C. S. and Lin, I. N., Microwave dielectric properties of glassceramic composites for low temperature co-firable ceramics. *J. Eur. Ceram. Soc.*, 2004, **24**, 1795–1798.
  4. Lo, C. L., Duh, J. G., Chiou, D. S. and Lee, W. H., Low-temperature sintering and microwave dielectric properties of anorthite-based glass-ceramics. *J. Am. Ceram. Soc.*, 2002, **85**(9), 2230–2235.
  5. Valant, M. and Suvorov, D., Microstructural phenomena in low-firing ceramics. *Mater. Chem. Phys.*, 2003, **79**, 104–110.
  6. Hunag, C. L., Weng, M. H., Lion, C. T. and Wu, C. C., Low temperature sintering and microwave dielectric properties of Ba<sub>2</sub>Ti<sub>9</sub>O<sub>20</sub> ceramics using glass additions. *J. Eur. Ceram. Soc.*, 2000, **35**, 2445–2456.
  7. Wang, S. H. and Zhou, H. P., Densification and dielectric properties of CaO–B<sub>2</sub>O<sub>3</sub>–SiO<sub>2</sub> system glass ceramics. *J. Mater. Sci. Eng.*, 2003, **B99**, 597–600.
  8. Cheng, C. C., Hsieh, T. E. and Lin, I. N., Microwave dielectric properties of glass-ceramic composites for low temperature co-firable ceramics. *J. Eur. Ceram. Soc.*, 2003, **23**, 2553–2558.
  9. Chang, C. R. and Jean, J. H., Crystallization kinetics and mechanism of low-dielectric, low-temperature, cofirable CaO–B<sub>2</sub>O<sub>3</sub>–SiO<sub>2</sub> glass-ceramics. *J. Am. Ceram. Soc.*, 1999, **82**(7), 1725–1732.
  10. Dernovsek, O., Naeini, A., Preu, G., Wersing, W., Eberstein, M. and Schiller, W. A., LTCC glass-ceramic composites for microwave application. *Mater. Res. Bull.*, 2001, **21**, 1693–1697.
  11. Eberstein, M., Schiller, W., Dernovsek, O. and Wersing, W., Adjustment of dielectric properties of glass ceramic composites via crystallization. *Glastech. Ber. Glass Sci. Technol.*, 2000, **73**(c1), 370–373.
  12. Kim, D. W., Hong, K. S., Yoon, C. S. and Kim, C. K., Low-temperature sintering and microwave dielectric properties of Ba<sub>5</sub>Nd<sub>4</sub>O<sub>15</sub>–BaNd<sub>2</sub>O<sub>6</sub> mixtures for LTCC applications. *J. Eur. Ceram. Soc.*, 2003, **23**, 2597–2601.
  13. Valant, M. and Suvorov, D., Glass-free low-temperature cofired ceramics: calcium germinates, silicates and tellurates. *J. Eur. Ceram. Soc.*, 2004, **24**, 1715–1719.
  14. Bain, J. J., Kim, D. W. and Hong, K. S., Microwave dielectric properties of Ca<sub>2</sub>P<sub>2</sub>O<sub>7</sub>. *J. Eur. Ceram. Soc.*, 2003, **23**, 2589–2592.
  15. Lu, C. H. and Huang, Y. H., Densification and dielectric properties of barium neodymium titanium oxide ceramics. *J. Mater. Sci. Eng.*, 2003, **B98**, 33–37.
  16. Yoon, S. H., Kim, D. W., Cho, S. Y. and Hong, K. S., Phase analysis and microwave dielectric properties of LTCC TiO<sub>2</sub> with glass system. *J. Eur. Ceram. Soc.*, 2003, **23**, 2549–2552.
  17. Chen, X. M., Sun, Y. H. and Zheng, X. H., High permittivity and low loss dielectric ceramics in the BaO–La<sub>2</sub>O<sub>3</sub>–TiO<sub>2</sub>–Ta<sub>2</sub>O<sub>5</sub> system. *J. Eur. Ceram. Soc.*, 2003, **23**, 1571–1575.
  18. Huang, C. L., Pan, C. L. and Shium, S. J., Liquid phase sintering of MgTiO<sub>3</sub>–CaTiO<sub>3</sub> microwave dielectric ceramics. *J. Mater. Chem. Phys.*, 2002, **78**, 111–115.